UNIVERSITY OF WATERLOO COMPUTER SCIENCE DEPARTMENT

Comparison of the Single Phase and Two Phase Numerical Model Formulation for Saturated-Unsaturated Groundwater Flow

Peter A. Forsyth

Research Report
CS-87-62

November, 1987

Comparison of the Single Phase and Two Phase Numerical Model Formulation for Saturated-Unsaturated Groundwater Flow

Peter A. Forsyth

Department of Computer Science
University of Waterloo
Waterloo, Ontario
N2L 3G1

ABSTRACT

Two numerical methods are developed for transient saturated-unsaturated two dimensional groundwater flow. One formulation uses the usual single phase formulation with a passive air phase at constant pressure. The second model uses a full two phase air-water formulation. The numerical results for both formulations are compared on some test problems. In some cases, the single phase formulation and the two phase formulations give greatly different results. This can be explained in terms of the fractional flow curve for the air-water system. The single phase technique generally requires less computational work than the two phase formulation, although there are some situations where the numerical performance of the single phase formulation is very poor.

1. Introduction

Since a groundwater system is generally open to the air, it is common practice to neglect the flow of the air phase, and assume that the pressure in the air phase is atmospheric [1-4]. This assumption effectively eliminates the air mass balance from a groundwater flow model.

The passive air phase assumption is also commonly used in numerical models of immiscible contaminant transport in groundwater systems [5-8]. Immiscible models are required for simulation of pollutant transport involving fuel oil, gasoline, or organic solvents. In general, simulation of non-aqueous phase organic components necessitates modelling of three phase flow: air, water and a non-aqueous phase. The constant air pressure assumption reduces the number of unknowns and equations by one.

In the context of saturated-unsaturated (air-water) groundwater flow problems, some authors have questioned the assumption of a passive air phase [9,10]. A one dimensional model of water infiltration into a soil column has been developed [10] which can use either the full two phase air-water formulation, or the usual single phase approach with a constant air pressure. In some circumstances, the two approaches give significently different results, with the two phase model predictions being closer to experimental results. [10] The authors also find that the two phase approach is computationally less expensive than the single phase method [10]. However, the model is one dimensional, which permits use of the simplifying assumption of constant total fluid velocity, and hence requires solution of only one equation for both approaches. This will not in general be possible in more than one dimension.

The objective of this article is to examine closely the assumption of a passive air phase in multi-dimensional groundwater systems. Attention is restricted to two phase air-water systems. Two separate numerical models are formulated, one using the full two phase approach, and the other using the standard single phase (constant air pressure) method. The numerical results for both models will be compared for some two-dimensional groundwater problems. The results are explained in terms of the shape of the fractional flow curves.

2. Formulation

The equations for two phase water (w) and air (a) flow in a porous medium are: [11]

Water mass balance:

$$\frac{\partial}{\partial t}(\phi S_w \rho_w) = q_w + \nabla \cdot \left[\frac{K K_{rw} \rho_w}{\mu_w} (\nabla P_w - \rho_w g \nabla D) \right] \tag{1}$$

Air mass balance:

$$\frac{\partial}{\partial t}(\phi S_a \rho_a) = q_a + \nabla \cdot \left[\frac{K K_{ra} \rho_a}{\mu_a} (\nabla P_a - \rho_a g \nabla D) \right] \tag{2}$$

where :

ϕ	=	porosity
S_ℓ	=	saturation of phase ℓ
ρ_ℓ	=	density of phase ℓ
$K_{r\ell}$	=	relative permeability of phase ℓ
P_ℓ	=	pressure of phase ℓ
μ_ℓ	=	viscosity of phase ℓ
g	=	gravitational acceleration
D	=	depth
q_ℓ	=	source/sink term for phase ℓ

Since the saturations sum to one, the air saturation is given by:

$$S_a = 1 - S_w \tag{3}$$

The air pressure is related to the water pressure through the capillary pressure P_{cwa} :

$$P_a = P_w + P_{cwa}\,(S_w) \tag{4}$$

The capillary pressure P_{cwa} is an experimentally determined function of water saturation [11], as are the relative permeabilities $K_{r\ell}$ [11]. The porosity is assumed to be the following function of water pressure P_w:

$$\phi = \phi_o\,[1 + C_m\,(P_w - P_o)] \tag{5}$$

where ϕ_o is the porosity at pressure P_o, and C_m is the compressibility of the porous medium. Normally C_m is very small.

The density of the water phase is given by:

$$\rho_w = \rho_{wo}\,[1 + C_w\,(P_w - P_o)] \tag{6}$$

where ρ_{wo} is the density of the water phase at pressure P_o. The density of the air phase is given by the ideal gas law:

$$\rho_a = \frac{\rho_{ao}\,P_a}{P_o} \tag{7}$$

where ρ_{ao} is the density of air at $P = P_0$.

For the purposes of this study, the viscosities will be assumed to be constants, although they are sometimes taken to be functions of phase pressures [7,8].

The system of equations (1-7) represents a set of two equations in the two primary variables P_w, S_w. All other variables are functions of these two unknowns. This set of equations represents

the full two phase approach to the solution of saturated-unsaturated groundwater flow.

However, if the air phase pressure is assumed to be constant, $P_a = \bar{P}_a$, then equation (4) can be used to eliminate the water saturation:

$$\bar{P}_a = P_w + P_{cwa}(S_w) \tag{8}$$

For example, suppose the capillary pressure is a straight line function of the water pressure:

$$P_{cwa} = P'_c\,(1 - S_w) \tag{9}$$

where P'_c is a constant. Then S_w is given by:

$$S_w = \min\left[1,\ 1 - \left(\frac{\bar{P}_a - P_w}{P'_c}\right)\right] \tag{10}$$

so that S_w is a function of P_w.

Equation (8) eliminates the water saturation as a primary variable, the only unknown being the water pressure P_w. This also implies that the air mass balance (equation (2)) can be dropped from the system of equations. Consequently, the single phase approach uses only equations (1) and (8) to give a system with one equation and one unknown.

It is immediately obvious that the single phase approach entirely ignores all flow properties of the air, in particular the relative permeability of the air phase is neglected.

3. Discretization

The discretized equations for the two phase approach will be given in the following. The single phase method uses a subset of the two phase equations along with equation (8).

The equations (1-2) are discretized in a cell centered finite difference form similar to that used in [5-8]. If N represents the time level, and i the i'th finite difference cell, then the discretized forms for equations (1-2) are:

Mass balance for phase $\ell = w, a$:

$$\frac{V_i}{\Delta t}\left[(\phi S_\ell \rho_\ell)_i^{N+1} - (\phi S_\ell \rho_\ell)_i^{N}\right] - q_{\ell i}^{N+1} \tag{11}$$

$$- \frac{V_i}{\Delta x_i}\left[T^M_{\ell\, i+\frac{1}{2}}\, K_{i+\frac{1}{2}}\, \psi_{\ell\, i+\frac{1}{2}} - T^M_{\ell\, i-\frac{1}{2}}\, K_{i-\frac{1}{2}}\, \psi_{\ell\, i-\frac{1}{2}}\right]$$

$$+ [y \text{ and } z \text{ flowterms}] = 0$$

where:

$V_i =$ volume of i'th finite difference cell

$$T_\ell = \frac{K_{r\ell}\, \rho_\ell}{\mu_\ell}$$

$\Delta x_i =$ cell width in the x-direction

$\psi_\ell =$ phase potential

The absolute permeability $K_{i+\frac{1}{2}}$ is defined using the harmonic mean [7], and $T_{\ell\, i+\frac{1}{2}}$ represents either $T_{\ell i}$ or $T_{\ell\, i+1}$ depending on the upstream point for phase ℓ [11]. The superscript M can be either the N'th or $(N+1)$'th time level (this will be discussed later). The phase potentials ψ_ℓ are given by:

$$\psi_{wi+\frac{1}{2}} = \frac{P^{N+1}_{wi+1} - P^{N+1}_{wi}}{(\Delta x_i + \Delta x_{i+1})/2} \tag{12}$$

$$- \frac{(\Delta x_i \rho^M_{wi+1} + \Delta x_{i+1}\rho^M_{wi})}{(\Delta x_i + \Delta x_{i+1})} \quad \frac{(D_{i+1} - D_i)}{(\Delta x_i + \Delta x_{i+1})/2}$$

$$\psi_{ai+\frac{1}{2}} = \frac{P^{N+1}_{wi+1} - P^{N+1}_{wi}}{(\Delta x_i + \Delta x_{i+1})/2} + \frac{P^M_{cwai+1} - P^M_{cwai}}{(\Delta x_i + \Delta x_{i+1})/2}$$

$$- \frac{(\Delta x_i \rho^M_{ai+1} + \Delta x_{i+1}\rho^M_{ai})}{(\Delta x_i + \Delta x_{i+1})} \quad \frac{(D_{i+1} - D_i)}{(\Delta x_i + \Delta x_{i+1})/2}$$

The equations (11-12) are implicit in the water pressure P_w, except for the weak dependence in the density terms. Expressions which are functions of S_w and P_w in the flow (pressure gradient) terms are implicit or explicit depending on whether $M=N$ or $M=N+1$. If cell i is a fully implicit cell, then $M=N+1$. If cell i is an IMPES cell (implicit pressure, explicit saturation) [11], then $M=N$. The state of a cell (fully implicit or IMPES) can change dynamically during the course of a simulation. Switching criteria are based on stability considerations. This adaptive implicit method is described in detail in references [12,13,14]. The adaptive implicit method achieves the stability of a fully implicit method while using much less work and storage than a fully implicit method.

Ignoring for the moment the use of upstream weighting in equations (11-12), then a standard tayler series truncation error analysis shows that the spatial error is of $0(\Delta x^2)$ if $\Delta x_i =$ constant. If Δx_i is spatially varying (an irregular-grid) then the truncation error is formally 0(1) (non-convergent). However, some more recent work has shown that a cell centered discretization is $0(max(\Delta x_i)^2)$ even for an irregular grid [15,16]. Of course, use of

upstream weighting results in a first order truncation error in equations (12-13). The error in the time direction is also first order.

The discretized equations are solved using full Newton iteration, and an iterative method based on an incomplete LU factorization with ORTHOMIN acceleration is used to solve the Jacobian [13,17]. Full advantage is taken of the sparsity structure of the adaptive implicit Jacobian (i.e., no zeros are stored or multiplied).

The above numerical method applies to the full two phase approach. In the single phase method, only the water equation is used, with the water saturation given by equation (8). The single unknown P_w is taken to be fully implicit in all flow terms ($M=N+1$ in equation (13)). Again, full Newton iteration is used to solve for P_w^{N+1}. Since there is only one unknown per cell in the single phase method, this technique will require less work in work general than the two phase approach.

4. Fractional Flow Curves

Before examining some test problems, it is instructive to consider some simple cases of equations (1-2). Assuming one dimensional flow with no gravity or source/sink terms, then:

$$\frac{\partial}{\partial t}(\rho_w S_w \phi) + \frac{\partial}{\partial x}(\rho_w V_w) = 0 \tag{13}$$

$$\frac{\partial}{\partial t}(\rho_a S_a \phi) = \frac{\partial}{\partial x}(\rho_a V_a) = 0 \tag{14}$$

where V_ℓ is the velocity of phase ℓ. If the water water phase is incompressible and pressure changes in the air phase are small, then equations (13) and (14) can be approximated by [10].

upstream weighting results in a first order truncation error in equations (12-13). The error in the time direction is also first order.

The discretized equations are solved using full Newton iteration, and an iterative method based on an incomplete LU factorization with ORTHOMIN acceleration is used to solve the Jacobian [13,17]. Full advantage is taken of the sparsity structure of the adaptive implicit Jacobian (i.e., no zeros are stored or multiplied).

The above numerical method applies to the full two phase approach. In the single phase method, only the water equation is used, with the water saturation given by equation (8). The single unknown P_w is taken to be fully implicit in all flow terms ($M=N+1$ in equation (13)). Again, full Newton iteration is used to solve for P_w^{N+1}. Since there is only one unknown per cell in the single phase method, this technique will require less work in work general than the two phase approach.

4. Fractional Flow Curves

Before examining some test problems, it is instructive to consider some simple cases of equations (1-2). Assuming one dimensional flow with no gravity or source/sink terms, then:

$$\frac{\partial}{\partial t}(\rho_w S_w \phi) + \frac{\partial}{\partial x}(\rho_w V_w) = 0 \tag{13}$$

$$\frac{\partial}{\partial t}(\rho_a S_a \phi) = \frac{\partial}{\partial x}(\rho_a V_a) = 0 \tag{14}$$

where V_ℓ is the velocity of phase ℓ. If the water water phase is incompressible and pressure changes in the air phase are small, then equations (13) and (14) can be approximated by [10].

$$\frac{\partial}{\partial t}(S_w \phi) = K V_t \frac{\partial}{\partial x}(f_w) \tag{15}$$

where:

$$V_t = V_a + V_w = \text{constant} \tag{16}$$

$$f_w = \frac{\dfrac{K_{rw}}{\mu_w}}{\dfrac{K_{rw}}{\mu_w} + \dfrac{K_{ra}}{\mu_a}}$$

Here f_w is the fractional flow curve, and capillary effects have also been neglected in equation (15). Complete details of the approximations involved are given in reference [10].

Equation (15) is a non-linear first order hyperbolic equation for S_w. Some example fractional flow curves for various types of relative permeabilities are shown in Figure 1. It has been assumed that:

$$\frac{\mu_w}{\mu_a} = 100$$

which is a typical value. For non-linear hyperbolic systems, it is generally expected that shocks and rarefactions can form [18]. Equation (15) is a form of the well known Buckley-Leverett equation [19].

Consider the following initial condition. Suppose the flow is in the positive x-direction ($V_t > 0$ in equation (15)), with an initial state of $S_L = 1$ for $x \leq 0$, and $S_R = 0$ for $x > 0$. Equation (15) will describe the time evolution of this system. Satisfaction of the generalized entropy condition [18] requires that physically admissable solutions to equation (15) obey a geometric constraint with respect

to the fractional flow curve f_w (Figure 1). For the fractional flow curves shown in Figure 1, this constraint can be stated as follows: the chord connecting the state on the right ($S_R=0$) to the state on the left ($S_{L)}$ must lie above f_w. This chord is shown as the dotted line in Figure 1. Figure 1a was constructed assuming:

$$K_{ra} = S_a, K_{rw} = S_w$$

Figure 1b was constructed assuming:

$$K_{ra} = S_a^2, K_{rw} = S_w^2$$

while Figure 1c was constructed assuming:

$$K_{ra} = S_a^4, K_{rw} = S_w^4$$

In the case of Figure 1a and 1b, the chord construction indicates that the initial shock of unit height will continue to propagate to the right ($S_L=1$). However, if the fractional flow curve is similar to Figure 1c, then the chord construction intersects the fractional flow curve f_w at a value of S_w less than one. This value $S_w=S_s$ is given by the point on the x-axis where the chord from $S_w=0$ is tangent to f_w (see Figure 1c). Consequently, the system will form a rarefaction fan with values $S_s<S_w<1$, followed by a shock of height S_s.

Suppose that the single phase approach is being used to model the time evolution of the system with the initial conditions described above

$$S_w=1,\ x\leq 0;\ S_w=0,\ x>0.$$

Consider the i-th finite difference cell, with

$$S_{wi} = S_{wi+1} = \cdots = 0;\ S_{wi-1} = S_{wi-2} = \cdots = 1.$$

If the capillary effects are small, of $0(\epsilon)$, then the initial pressures will be:

$$P_i = P_{i+1} = \cdots = \bar{P}_a - \epsilon$$

$$P_{i-1} = P_{i-2} = \cdots = P \geq \bar{P}_a$$

where $\bar{P}$ is the constant atmospheric pressure. Equation (8) implies that

$$\bar{P}_a - \epsilon < P_i < \bar{P}_a,\ 0 < S_{wi} < 1$$

This means that there will be very little flow from cell i to cell $i+1$ (due to the small pressure gradient) until cell i fills up with water. Thus, the single phase approach, at least for this simple case, will tend to propagate sharp shock fronts of unit height.

For fractional flow curves as given by Figures 1a and 1b, the true two phase solution also has shock fronts of unit height. In these cases, we can expect that the single phase solution and the two phase solution will be in good agreement. However, in the case of an f_w similar to Figure 1c, the true two phase solution consists of a rarefaction behind a shock. Since the single phase solution uses no information about the air relative permeability curve, the single phase technique will tend to propagate a shock of unit height, with no rarefaction. In this situation, we can expect significant deviation between the single phase and the two phase solutions.

Note that the shock formation for the air-water system is enhanced by the large viscosity ratio (μ_w/μ_a) which strongly influences the shape of the fractional flow curves.

Of course, it remains to be seen whether the above highly simplified analysis is applicable to multi-dimensional flows where gravity and capillary effects are important. This will be investigated by means of some numerical examples.

5. Dam Seepage Problem

In order to verify that the single phase model and the two phase model are giving results comparable to previously published solutions, the first example is the well known dam seepage problem [20,21,22]. Although this is a steady-state problem, the time dependent equations (11-12) can be used by starting with an arbitrary initial state and integrating to a large time.

The geometry for this example is given in Figure 2, and consists of a rectangular porous dam with a headwater of height h_1, a tailwater of height h_2 and base length ℓ. A full description of this problem and a complete bibliography is available in [21]. Many different numerical techniques have been used to solve this problem [21], but to the best of my knowledge a full two phase solution has not been attempted previously.

The data used for this example are given in Table 1. The height of the seepage point h_s is only dependent on the ratios of h_1, h_2 and ℓ. However, for completeness, all the physical data are shown in Table 1.

The region $ABCF$ in Figure 2 was discretized using a regular cell centered grid. Half cells were used on the boundaries, so that cell centers coincided exactly with the boundaries. Initially, the dam was unsaturated ($S_w=0$).

Since only the steady state solution was of interest, the following computational procedure was adopted. With $S_w=0$ at $t=0$, a coarse 5×7 grid was used initially. The equations were integrated to a time of two years, at which time the saturation changes were very small. The solution on this coarse grid was then interpolated onto a finer grid (cell size halved in the x and y directions), the time integration was repeated, the results interpolated onto a finer grid, and so on. The mesh sequence consisted of 5×7, 9×13, 17×25 and 33×49 grids. An initial timestep size of .01 days was used on each grid, and a timestep selector based on saturation changes [13] was used. Timesteps built up very rapidly, typically the entire two years was completed in about 10 timesteps. For the two phase formulation, each grid was initialized so that all cells were in the IMPES state (only one unknown per cell for the Jacobian solver). On the finest grid, saturation changes of the order of 10^{-5} were observed over the final one year timestep, indicating that for practical purposes, the system had reached a steady state.

The boundary conditions for the two phase method were defined as follows: along AB (Figure 2) the water pressure was specified by the head of water:

$$P^* = \max\,[0,\ \rho_w g\ (D-D_1)] + \bar{P}_a$$

where D_1 is the depth to the water surface on AB. This pressure was fixed by injecting water into the boundary cells with a source term of the form:

$$q_w = W_i\,(P^*-P_{wi}) \tag{17}$$

where P_{wi} is the pressure in the i'th boundary cell, and W_i is a large number selected so that

$$|P^*-P_{wi}| << P^*$$

The boundary BC is a no-flow boundary, while CD has a pressure specified by the head of water in the tailwater:

$$P^* = \max[0, \rho_w g (D-D_2)] + \bar{P}_a$$

where D_2 is the depth to the top of the tailwater. Consequently, along CD, a constant pressure sink term of the form:

$$q_w = \frac{K K_{rw}}{\mu_w} W_i (P^*-P_{wi})$$

is used.

Along DF, a constant air pressure $\bar{P}_a$ is specified. This boundary condition is imposed by sink terms of the form:

$$q_w = \frac{K K_{rw}}{\mu_w} W_i (\bar{P}_a-P_{wi}), \qquad (\bar{P}_a-P_{wi}) < 0 \tag{18}$$

$$= 0 \qquad , (\bar{P}_a-P_{wi}) > 0$$

$$q_a = \frac{K K_{ra}}{\mu_a} W_i (\bar{P}_a-P_{ai})$$

Note that the above sign check for q_w ensures that seepage occurs only when the water pressure is greater than the atmospheric pressure $\bar{P}_a$.

Along AF, air was injected at pressure $\bar{P}_a$:

$$q_a = W_i (\bar{P}_a-P_{ai}) \tag{19}$$

The capillary pressure for the two phase runs was set equal to zero ($P_c'=0$, so that $P_w=P_a$).

Turning to the single phase formulation, a finite size capillary pressure must be used, otherwise the equations for the water saturation (equations (8-10)) become indeterminate. Given a finite

P_c' (Table 1, equations (9-10)), then the initial water pressure is set to be:

$$P_w = \bar{P} - P_c' \tag{20}$$

to give a zero water saturation in the dam. The boundary condition along AB was specified using equation (17), while BC was a no-flow boundary. On CD, the same constant pressure sink term was used as for the two phase method.

Along DF, the same water sink term as in equation (18) was used. Since there is no air phase in this formulation, a constant air pressure cannot be specified along AF. However, in practice, the top row of cells is never saturated, so that water does not flow across AF (since the water pressure is less than atmospheric). Consequently, a no-flow boundary condition is applied to AF.

In order to compare the single phase and the two phase techniques, a consistent method of estimating the height of the seepage point h_s (Figure 2) is required. The following method was selected: h_s is the distance from the base of the dam to the top of the highest cell (along CF) with $S_w = 1.0$. In the single phase case no seepage can occur if $S_w < 1.0$. This is because a finite capillary pressure implies that $P_w < \bar{P}_a$ if $S_w < 1$, and hence no flow from equation (18). In the two phase situation, since the capillary pressure is zero, two phase seepage can occur. However, the water seepage q_w is very small in any cell with $S_w < 1.0$, since the air viscosity is much smaller than the water viscosity. As the water saturation decreases from unity to zero in 2-3 cells in the vertical direction (for small capillary pressure), any other reasonable method for selecting the seepage point will adjust this distance by at most half a cell width.

The results for the height of the seepage point h_s are shown

in Table 2. For comparison, we also give the result obtained in [21] using an integral equation method. This result [21] was scaled to correspond to the physical dimensions and used in this study.

Note the excellent agreement between the single phase method with $P_c'=1\,kpa$, and the two phase approach on the 33×49 grid. As noted previously, the single phase formulation requires a finite size capillary pressure, but a capillary pressure of the form in Table 1 with $P_c'=1\ kpa$ gives a capillary fringe of about .1 m. This cannot be resolved on the finest grid (cell size 1.25 m). A capillary fringe of approximately 1 m can be expected with $P_c'=10\ kpa$. From Table 2, the single phase method with $P_c'=10\ kpa$ appears to be converging to a seepage point about 1 m higher than the runs with $P_c'=1\ kpa$, consistant with physical reasoning.

Upstream weighting of the relative permeability is used for both the single phase and two phase approaches. Upstream weighting is necessary in the two phase case since the system is hyperbolic-parabolic, and upstream weighting ensures convergence to the correct physical solution [19] In the single phase case, upstream weighting ensures that the saturation profile decreases monotonically from one to zero in the vertical direction.

The small capillary pressure results for both single phase and two phase formulations are in good agreement with the calculation carried out in [21], which is believed to be correct to the number of figures shown. In view of the fact that there is some degree of uncertainty in the experimental capillary curves, even the coarse 17×25 grids are probably adequate for practical purposes.

Since the derivative of equation (10) is discontinuous at $S_w=1.0$, it was found necessary to underrelax the Newton iteration for the single phase formulation whenever a cell switched from the saturated state to the unsaturated state or vice versa. The single phase approach was approximately 2-3 times faster, in terms of

CPU time, than the two phase method.

It does not appear possible to solve the dam seepage problem using the single phase formulation with a value of P_c' much less than than $1\ kpa$. Smaller values of P_c' caused an excessive number of Newton iterations, and many timestep cuts. Consequently, the single phase method may have some difficulty in modelling problems with a very small capillary pressure.

To investigate the effect of non-linear relative permeability curves on the performance of these methods, several runs were carried out with quadratic relative permeability curves. Only slight differences of the order of the truncation error were observed in the results. However, for small values of the capillary pressure, the single phase method required a large number of Newton iterations for convergence. This is shown in Table 3. The numerical performance of the two phase formulation was relatively unaffected by non-linear relative permeability curves. In fact, the CPU time for the single phase formulation was comparable with the CPU time for the two phase method in this case.

Since the water pressure in the single phase formulation is tightly coupled to the water saturation by equation (10), it is clear that increasing the non-linearity of K_{rw} causes Newton's method some difficulty. In the two phase method, the pressure and saturation are comparatively weakly coupled, so that Newton's method has less difficulty with a non-linear K_{rw}. A similar effect has been observed in thermal oil reservoir simulation [23] where the use of extra unknowns (and equations) enhances the convergence of Newton's method.

In the case of the two phase formulation, the adaptive implicit method proved quite effective. Only a small number of cells near the saturated-unsaturated transition zone turned fully implicit during the course of the run.

6. Time Dependent Example

In order to determine the effect of different fractional flow curves on the time dependent results for the single phase and two phase methods, consider the example illustrated in Figure 3. The data used for this problem are given in Table 4. The region $ABCDE$ (Figure 3) is initially filled with air. As before, a cell centered [11] grid is used with half cells on the boundaries.

The boundary conditions for the two phase formulation were imposed as follows: along AB and AE a constant pressure ($P_a = 100\ kpa$) air source term is used to impose constant air pressure, while along BC a water source term is used, with water pressure P^* given by the static water pressure. The boundary CD is a no-flow boundary, while constant air pressure is imposed on DE by using constant pressure ($\bar{P}_a = 100\ kpa$) water and air sink terms. These source/sink terms have the same form as discussed for the Dam Seepage problem.

Turning attention to the single phase technique, the boundary conditions are specified in the following way: along BC a water source term is applied to force the correct pressure, CD is a no-flow boundary, while along DE, a water sink term is used with P_a a constant air-pressure $\bar{P}_a$. As with the Dam Seepage problem, we cannot specify air injectors along AB and AE, and so no-flow boundaries are imposed. In practice, since the capillary fringe does not extend past AE ($P_c' = 10\ kpa$ implies a fringe of about 1 m), these boundary cells along AB and AE are never saturated, and hence water cannot flow across these boundaries.

All sink terms for both single and two phase formulations involve a sign check to ensure that water seepage occurs only if water pressure is greater than atmospheric.

Several example runs were carried out with 11×11 and 21×21 regular grids. In order to provide a quantitative measure

of the difference between the two methods, we will consider the quantity:

$$Q = \frac{\sum_i V_i \phi_i S_{wi}}{\sum_i V_i \phi_i} \tag{21}$$

where the sum is over all cells. The dimensionless storage Q is the fraction of the available pore volume of the porous medium that is filled with water. Clearly, if there is a large difference in the computed value of Q, then there is a significant difference between the two approaches. Table 5 gives the results for the dimensionless storage Q at $t=1.0$ days. From Table 5, the spatial truncation error is of the order of 1-2 % for the 21×21 grid. This level of accuracy will be adequate to determine if there are any significant differences between the single phase and two phase methods. Consequently, all results reported in the following use the 21×21 grid.

The initial timestep size was .01 days, and a timestep selector based on saturation changes was used [13]. Small timesteps were required initially because of the extremely rapid water movement ($S_w=0.0$ initially) across the boundary BC. Several test runs were carried out with parameters that forced smaller timesteps from the timestep selector. The dimensionless storage changed only in the third decimal place, which is adequate for our purposes. A global material balance for the water was also monitored. At the end of the simulations, the global material balance error was less than 10^{-5}.

The dimensionless storage as a function of time is shown in Figure 4, ($K_{rw}=S_w$, $K_{ra}=S_a$), Figure 5 ($K_{rw}=S_w^2$, $K_{ra}=S_a^2$), and Figure 6 ($K_{rw}=S_w^4$, $K_{ra}=S_a^4$). The single phase and two phase formulations are in excellent agreement for both straight line and quadratic relative permeability curves. However, the fourth

power curves (Figure 6) show a large disagreement. In fact, at $t=1.0$ days, the single phase dimensionless storage is in error by 30%.

These results can be explained with reference to the fractional flow curves as shown in Figure 1. As discussed in Section 4, the fractional flow curves for an air-water system with straight line or quadratic relative permeability curves indicate that an initial shock of unit height will continue to propagate (Figure 1a, 1b). On the other hand, fourth power relative permeabilities will result in the evolution of a rarefaction followed by a shock from an initial shock of unit height.

Detailed examination of the output revealed that for fourth power relative permeability curves, the two phase solution did show a long rarefaction followed by a shock, while only a shock was observed for the single phase solution. This gives rise to the large discrepancy between the single phase and two phase formulations as shown in Figure 6. The word shock is used loosely here, since there is a non-zero capillary pressure which spreads the "shock" over several cells. As discussed in Section 4, the single phase formulation has a tendency to propagate sharp fronts. From Figure 6, it is clear that the amount of water stored in the porous medium is much larger for the single phase solution that for the two phase solution. The long rarefaction produced by the two phase method reduces the amount of fluid retained by the porous medium. This storage effect could be significant in practical problems.

Another measure of the difference between the single phase and diphasic formulations is given by the quantity:

$$\sum_{i=1}^{N} \frac{| S_{wi}^{S} - S_{wi}^{D} |}{N} \tag{22}$$

where N is the total number of cells, S_{wi}^{S} is the value of the saturation obtained with the single phase techniques, and S_{wi}^{D} is the same value obtained with the double phase formulation. Table 6 shows the average absolute saturation difference (equation (22)) at one day for the various relative permeability curves. As expected from Figures 4, 5, 6, there is a large deviation for the quartic curves. The differences are especially pronounced near the saturation front.

The shape of the fractional flow curve in Figure 1c is determined primarily by the flatness of the air relative permeability near $S_a=0$. To verify that the shape of K_{ra}, and hence the shape of the fractional flow curve, strongly affects the numerical results, a two phase simulation was carried out with $K_{rw}=S_w^4$, $K_{ra}=S_a$. This run was in good agreement with the single phase solution with $K_{rw}=S_w^4$.

In terms of CPU time, the single phase formulation was approximately 2-4 times faster than the two phase simulation (depending on the relative permeability curves), even for highly non-linear K_{rw}. This is in contrast to the Dam Seepage problem, where non-linearity causes slow convergence in the single phase method. However, for this example, the capillary fringe is of the order of 1 m thick, while the finite difference cells are .25 m in size. This gives a smooth transition between saturated ($S_w=1.0$) and completely unsaturated ($S_w=0.0$) cells in the vertical direction. In the case of the Dam Seepage problem, convergence difficulties were severe only in the case of a small capillary pressure, when the capillary fringe was less than a finite difference cell in length. Of course, a large P_c' also decreases the magnitude of the derivative with respect to P_w in equation (10), and hence

decreases the discontinuity in slope at $S_w = 1.0$.

7. Conclusions

Two separate numerical methods for saturated-unsaturated groundwater flow have been developed: the usual single phase formulation with a passive air phase at constant pressure, and a full two phase formulation. In the case of the dam seepage problem, both methods are in good agreement with each other and with previously published results.

For general time dependent flow problems, the single phase and two phase formulations agree as long as the relative permeability to air is not too flat near $S_a = 0$. If the relative permeability to air behaves like S_a^4 or a higher power near $S_a = 0$, then very large errors are observed in the single phase formulation. These results can be explained with reference to the air-water fractional flow curves.

In general, the single phase numerical model was several times faster (in terms of CPU time) than the two phase model. However, in the case of highly non-linear water relative permeability curves and finite difference cells larger than the capillary fringe, the numerical performance of the single phase formulation degraded to such an extent that it was no longer any faster than the two phase formulation.

To summarize, in many practical situations, the assumption of a passive air phase will give results very similar to a full two phase formulation with substantially less computational work. However, if the length of the capillary fringe is less than the length of a grid cell, or if the air relative permeability is very flat near $S_a = 0$, then the two phase formulation is preferred.

References

[1] J. Bear, *Dynamics of Fluids in Porous Media,* Elsevier, New York, 1972

[2] R.A. Freeze, "Three dimensional transient, saturated-unsaturated flow in a groundwater basin", Water Resour. Res. *7* (1971) 347-366.

[3] R.A. Freeze and J.A. Cherry, *Groundwater,* Prentice Hall, New Jersey, 1979.

[4] F.A. Dullien, *Porous Media Transport and Pore Structure,* Academic, New York, 1979.

[5] L.M. Abriola and G.F. Pinder, "A multi-phase approach to modelling of porous media contamination by organic compounds 1. Equation development", Water Resour. Res. *21* (1985) 11-18.

[6] L.N.M. Abriola and G.F. Pinder, "A multiphase approach to modelling of porous media contamination by organic compounds 2. Numerical simulation", Water Resour. Res. *21* (1985) 19-26.

[7] C.R. Faust, "Transport of immiscible fluids within and below the unsaturated zone: a numerical model", Water Resour. Res. *21* (1985) 587-596.

[8] G.F. Pinder and L.M. Abriola, "On the simulation of nonaqueous phase organic compounds in the subsurface", Water Resour. Res. *22* (1985) 1095-1195.

[9] D.W. Green, H. Dabiri and C.F. Weinaug, "Numerical modelling of unsaturated groundwater flow and comparison of the model to a field experiment", Water Resour. Res. *6* (1970) 862-874.

[10] H.J. Morel-Seytoux and J.A. Billica, "A two phase numerical

model for prediction of infiltration: applications to a semi-infinite column", Water Resour. Res. *21* (1985) 607-615.

[11] D.W. Peaceman, *Fundamentals of Numerical Reservoir Simulation,* Elsevier, New York, 1977.

[12] G.W. Thomas and D.H. Thurnau, "Reservoir simulation using an adaptive implicit method", Soc. Pet. Eng. J. *23* (1983) 760-768.

[13] P.A. Forsyth and P.H. Sammon, "Practical considerations for adaptive implicit methods in reservoir simulation", J. Comp. Phys. *62* (1986) 265-281.

[14] P.A. Forsyth and P.H. Sammon, "Local mesh refinement and modelling of faults and pinchouts", Soc. Pet. Eng. J. Form. Eval. *1* (1986) 275-285.

[15] T.A. Manteuffel and A.B. White, "The numerical solution of second order boundary value problems on non-uniform meshes", Los Alomos National Lab Preprint LA-UR-84-196, 1984.

[16] P.A. Forsyth and P.H. Sammon, "Quadratic convergence for cell centered grids", Appl. Num. Math. (to appear) 1987.

[17] A. Behie and P.A. Forsyth, "Incomplete factorization methods for fully implicit simulation of enhanced oil recovery", SIAM J. Sci. Stat. Comp. *5* (1984) 543-561.

[18] P.D. Lax, *Hyperbolic Systems of Conservation Laws and the Mathematical Theory of Shock Waves,* SIAM Regional Conference Series in Applied Mathematics, SIAM, Philadelphia, 1973.

[19] L.P. Dake, *Fundamentals of Reservoir Engineering,* Elsevier, New York, 1978.

[20] P. Ya Polubarinova-Kochina, *Theory of Groundwater Movement*, Princeton University Press, Princeton, 1962.

[21] C.W. Cryer, "A survey of steady state porous flow free boundary problems", M.R.C. Tech. Rep. 1657, Mathematics Research Center, Univ. of Wisconsin, 1976.

[22] D.R. Westbrook, "A mixed variational inequality boundary iteration method for some free boundary problems" SIAM J. Sci. Stat. Comp. *5* (1984) 192-202.

[23] P.A. Forsyth, B. Rubin and P.K.W. Vinsome, "Elimination of the constraint equation and modelling of some problems with a non-condensible gas in steam simulation", J. Can. Pet. Tech. *20* #4 (1981) 63-68.

TABLE 1

Data for the Dam Seepage problem.

Headwater height (h_1)	$60m$
Length (ℓ)	$40m$
Tailwater-height (h_2)	$10m$
Permeability	$10^{-11}\ m^2$
Porosity	0.3
Water viscosity	$1\ cp$ $(10^{-3}\ kg\ m^{-1}\ s^{-1})$
Air viscosity	$.01\ cp$ $(10^{-5}\ kg\ m^{-1}\ s^{-1})$
Water density ($P_w = 100\ kpa$)	$1000\ kg/m^3$
Air density ($P_a = 100\ kpa$)	$1.5\ kg/m^3$

Capillary pressure

$$P_{cwa} = P_c'(1 - S_w)$$

Relative permeabilities

$$K_{rw} = S_w \qquad K_{ra} = S_a$$

Atmospheric pressure	$100\ kpa$ $(10^5\ N\ m^{-2})$
Reference pressure	$100\ kpa$ $(10^5\ N m^{-2})$
Formation compressibility	$5\times10^{-6}\ kpa^{-1}$ $(5\times10^{-9}\ N^{-1}m^2)$
Water compressibility	$4.3\times10^{-7}\ kpa^{-1}$ $(4.3\times10^{-10}\ N^{-1}m^2)$

TABLE 2

Seepage point (h_2 in Figure 2) for the dam seepage problem.

Method	Grid	Maximum Capillary Pressure P_c' (Kpa)	$h_2(m)$
Two Phase	17×25	0.0	31.25
	33×49	0.0	31.875
Single Phase	17×25	10.0	33.75
	33×49	10.0	33.125
	17×25	1.0	33.75
	33×49	1.0	31.875
Integral Equation from Cryer [1976] (believed to be exact to figures shown)	N/A	0	31.875

TABLE 3

Effect of non-linear relative permeability on the single phase solution of the Dam Seepage problem, $P_c' = 1\,kpa$.

Relative Permeability	Total Number of Newton Iterations on the finest Grid
$K_{rw} = S_w$	26
$K_{rw} = S_w^2$	99

TABLE 4

Data for the time dependent example.

Permeability	$10^{-12} m^2$
Porosity	.3
Water Viscosity	1 cp
	$(10^{-3} kg\, m^{-1} s^{-1})$
Air Viscosity	.01 cp
	$(10^{-5} kg\, m^{-1} s^{-1}$
Water Density ($P_w = 100\ kpa$)	$1000 kg\, m^{-3}$
Air Density ($P_a = 100 kpa$)	1.5 $kg\, m^{-3}$
Capillary pressure	
$P_{cwa} = P_c'(1 - S_w)$	
$P_c' = 10 kpa$	
$(10^4 N m^{-2})$	
Relative Permeabilities	
$K_{rw} = S_w^{nw}$ $K_{ra} = S_a^{na}$	
Atmospheric Pressure	$\bar{P}_a = 100\ kpa$
	$(10^5 N m^{-2})$
Initial Water Saturation	$S_w = 0$
Initial Pressure	$P_w = 90 kpa\ (9 \times 10^4 N m^{-2})$
Formation Compressibility	$5 \times 10^{-6}\ kpa^{-1}$ $(5 \times 10^{-9} N^{-1} m^2)$
Water Compressibility	$4.3 \times 10^{-7}\ kpa^{-1}$ $(4.3 \times 10^{-10} N^{-1} m^2)$

TABLE 5

Dimensionless storage Q (fraction of pore volume filled with water) at $t=1.0$ days for different grid sizes. Quadratic relative permeability curves ($K_{rw}=S_w^2$, $K_{ra}=S_a^2$) used.

Method	Grid Size	Dimensionless Storage Q
Single Phase	11×11	.583
	21×21	.571
Two Phase	11×11	.570
	21×21	.563

TABLE 6

Average difference in computed water saturations for the single phase (S_{wi}^S) and double phase (S_{wi}^D) methods, $t = 1$ days.

Relative Permeability Used.	$\sum_{i=1}^{N} \frac{\lvert S_{wi}^S - S_{wi}^D \rvert}{N}$
$K_{rw} = S_w \quad K_{ra} = S_a$	.004
$K_{rw} = S_w^2 \quad K_{ra} = S_a^2$	.01
$K_{rw} = S_w^4 \quad K_{ra} = S_a^4$	.14

Figure Captions

(1) Fractional flow curves for air-water systems with:

(a) $K_{rw}=S_w$, $K_{ra}=S_a$

(b) $K_{rw}=S_w^2$, $K_{ra}=S_a^2$

(c) $K_{rw}=S_w^4$, $K_{ra}=S_a^4$

(2) Description of the region for the Dam Seepage problem.

(3) Illustration of the domain for the time dependent example.

(4) Dimensionless storage (fraction of pore volume filled with water) for the time dependent example, straight line relative permeabilities used ($n_a=n_w=1$).

(5) Dimensionless storage for the time dependent example, quadratic relative permeability curves ($n_a=n_w=2$).

(6) Dimensionless storage for the time dependent example, fourth power relative permeability curves ($n_a=n_w=4$).

FIGURE 1A

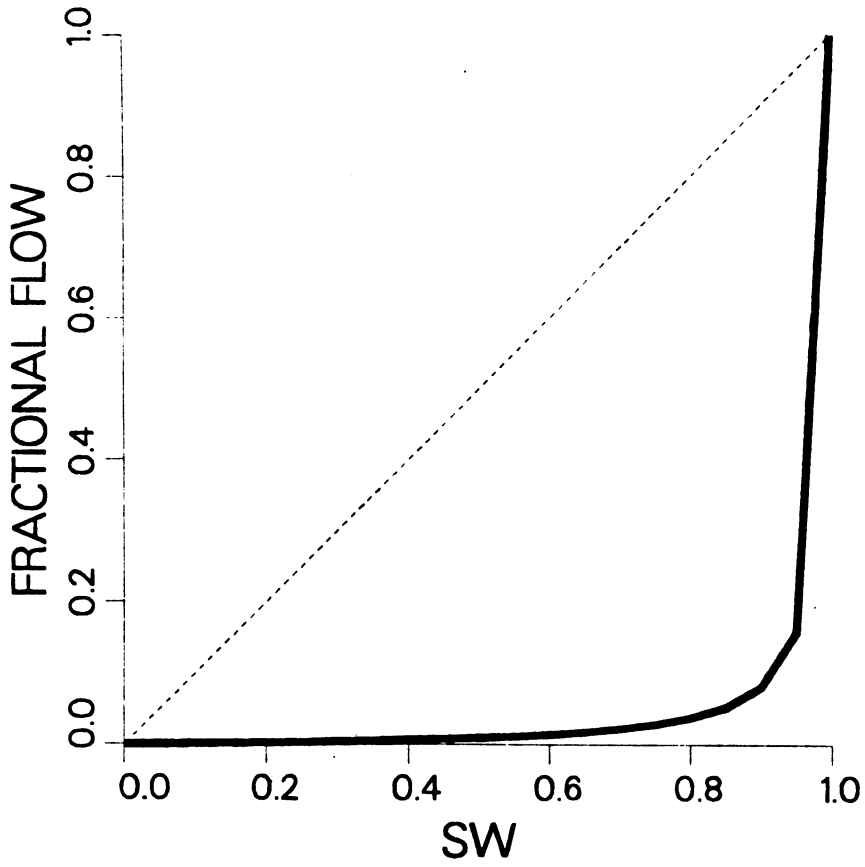

(1) Fractional flow curves for air-water systems with:

(a) $K_{rw} = S_w$, $K_{ra} = S_a$

FIGURE 1B

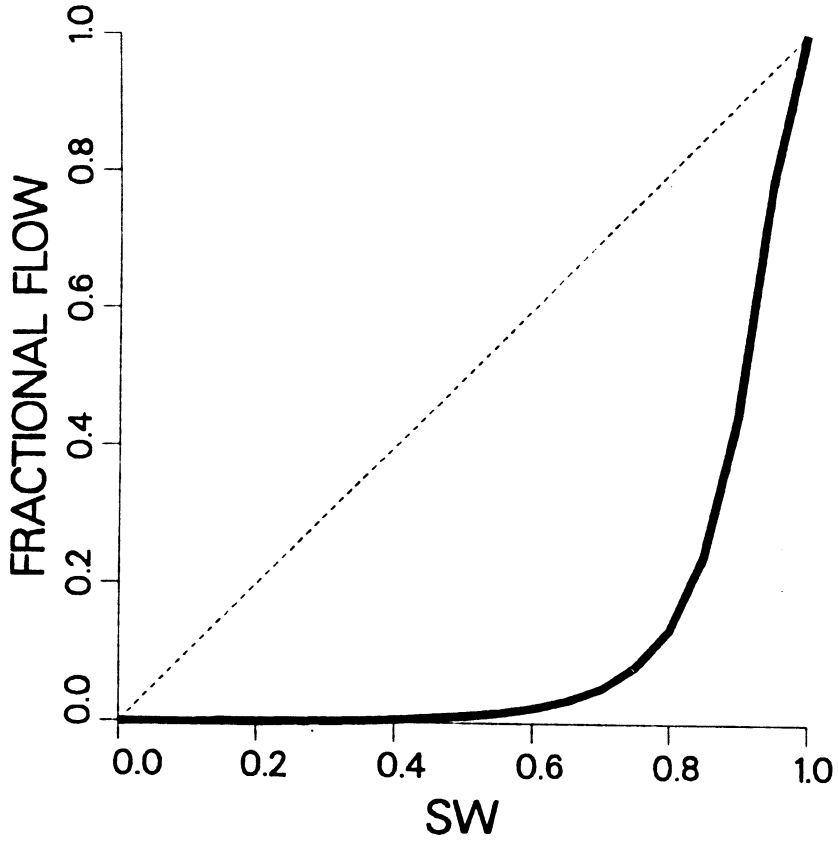

(1) Fractional flow curves for air-water systems with:

(b) $K_{rw}=S_w^2$, $K_{ra}=S_a^2$

FIGURE 1C

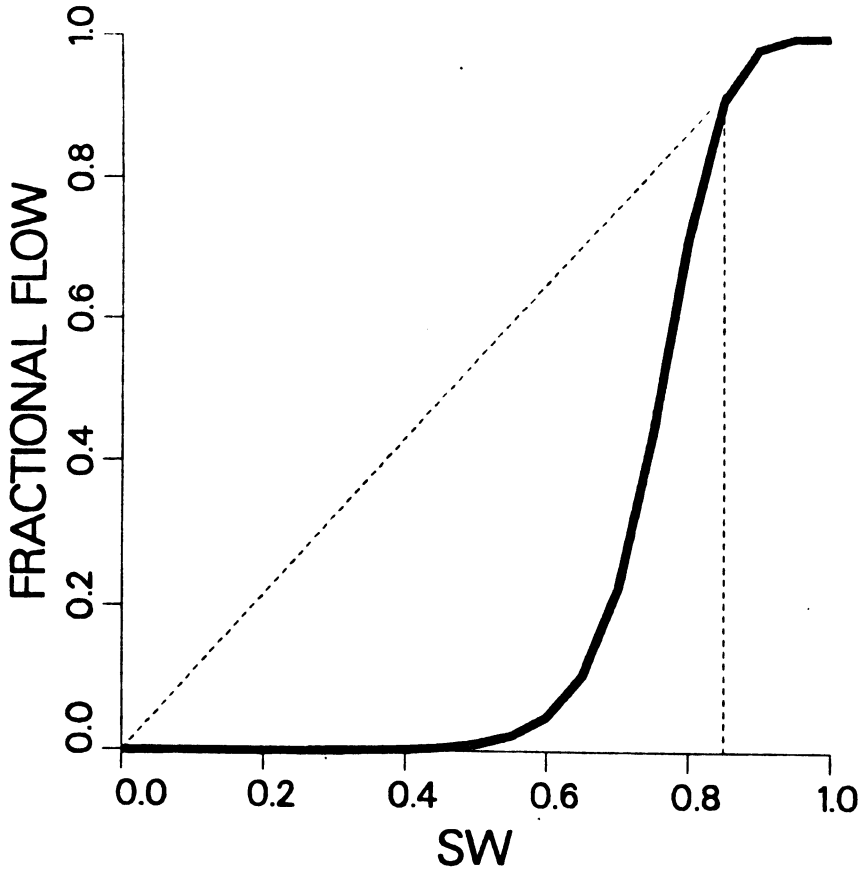

(1) Fractional flow curves for air-water systems with:

(c) $K_{rw} = S_w^4$, $K_{ra} = S_a^4$

FIGURE 2

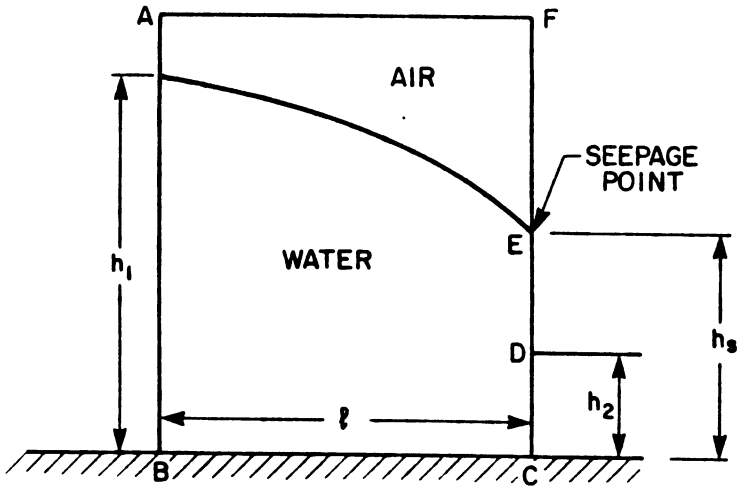

(2) Description of the region for the Dam Seepage problem.

FIGURE 3

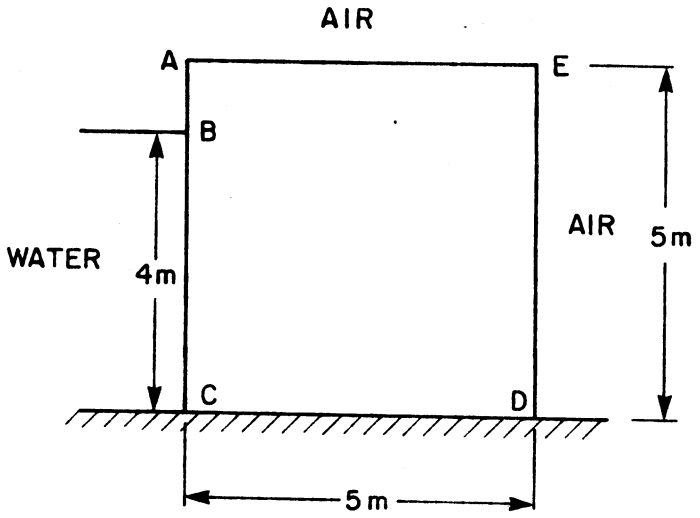

(3) Illustration of the domain for the time dependent example.

FIGURE 4

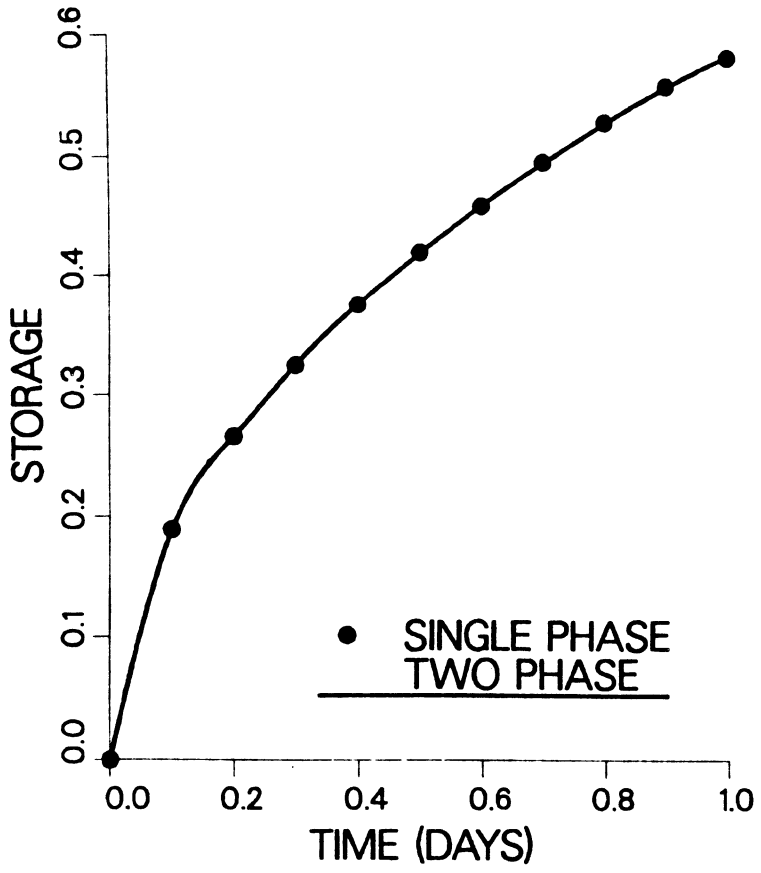

(4) Dimensionless storage (fraction of pore volume filled with water) for the time dependent example, straight line relative permeabilities used ($n_a = n_w = 1$).

FIGURE 5

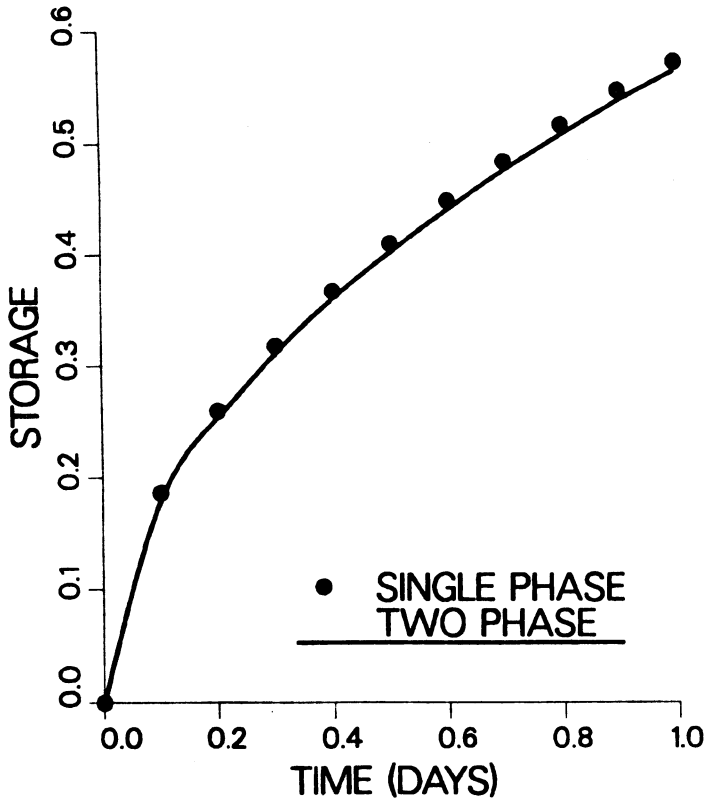

(5) Dimensionless storage for the time dependent example, quadratic relative permeability curves ($n_a = n_w = 2$).

FIGURE 6

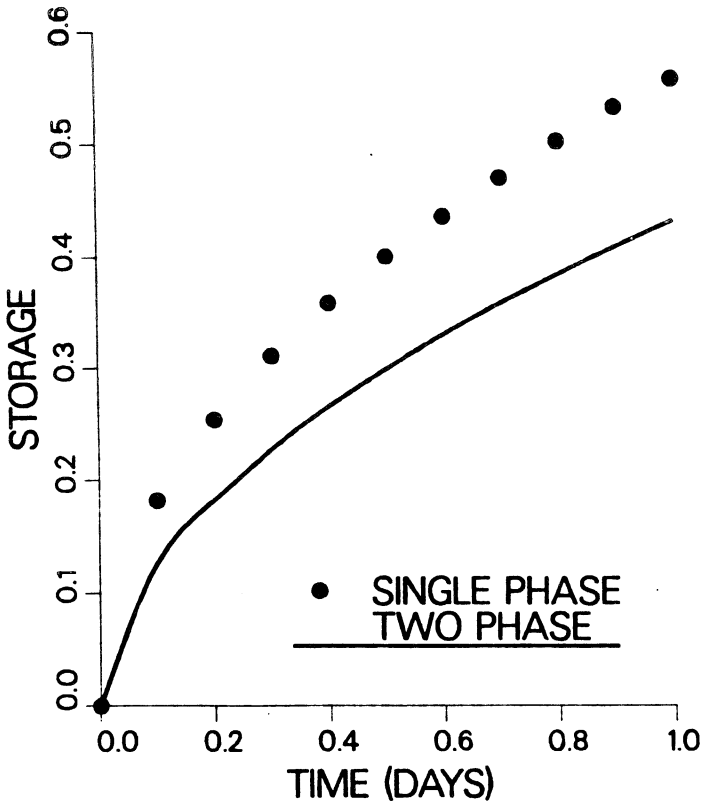

(6) Dimensionless storage for the time dependent example, fourth power relative permeability curves ($n_a = n_w = 4$).

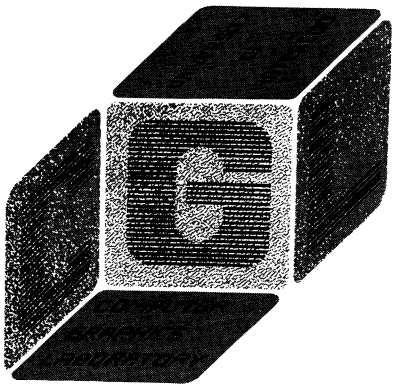

The Computer Graphics Laboratory at the University of Waterloo is a group of students and faculty doing research within the Computer Science Department. Interests include most areas of computer graphics, document preparation and man-machine interfaces. CGL is affiliated with the Institute for Computer Research. Graduate work at the masters and doctoral level leads to a Computer Science degree from the Faculty of Mathematics. Further information may be obtained by writing to the following address:

Computer Graphics Laboratory
University of Waterloo
Waterloo, Ontario, Canada N2L 3G1
(519) 888-4534